

29. SONG, C. W., M. S. KANZ, J. G. RHEE & S. H. LEVITT. 1979. Effect of hyperthermia on vascular function in normal and neoplastic tissues *in vivo*. Ann. N.Y. Acad. Sci. This volume.
30. DICKSON, J. A. & M. SUZANGAR. 1974. *In vitro-in vivo* studies on the susceptibility of the solid Yoshida sarcoma drugs and hyperthermia. Cancer Res. 34: 1263-1274.

DISCUSSION OF THE PAPER

LEON PARKS: We agree with Dr. Jain's conclusion regarding the importance of heating from within and heating by means of extracorporeal perfusion. He was eluded to its usefulness on a regional basis. In the past 18 months, we have induced whole-body hyperthermia by an extracorporeal approach.

KEVIN PARKER (*MIT, Cambridge, Mass.*): I would like to make some comments on our theoretical and experimental work, which is pertinent to Dr. Jain's presentation. This work was done in Dr. P. P. Lele's laboratory.

Localized hyperthermia can be produced in predetermined volumes of deep target tissue by insonation with one or more moving, focused beams of ultrasound. The level and distribution of the hyperthermia is governed, in part, by the local blood perfusion. Experimental results obtained in the brain of the cat and renal adenocarcinoma in the flank of the rat, *in vivo* and after circulatory arrest, were found to correlate well with those of a predictive heat transfer model based on the so-called bio-heat transfer equation. To test the validity of the model in predicting temperature distributions, hyperthermia of 5°C was produced in a doughnut-shaped volume of normal or tumor tissue in the anesthetized animal. The temperature distribution was measured by stepping calibrated thermocouples through the region of interest. The measurements were repeated after the animal was killed by an overdose of the anesthetic. The results obtained in the brain with a circular insonation trajectory, 2 cm in diameter, are shown in FIGURE D1. Note that with blood flow, the temperature drops off steeply in both directions from the region of energy deposition, producing a "dip" in the center. The spatial fall-off of temperature is less steep and the central dip is almost eliminated when blood flow ceases.

A predictive model incorporating the bio-heat transfer or Penne's equation can be used either to calculate spatially averaged perfusion rates from the results of the above experiments, or for predicting changes in temperature distributions *in vivo* from data obtained *in vitro*.

Briefly, the model assumes that the insonation creates a temperature "forcing function" along its axis with highest temperatures occurring in the focal plane.

FIGURE D2 depicts the model geometry, where the z axis corresponds to the axis of insonation, and the width $R_2 - R_1$ roughly corresponds to the diameter of the focal lobe.

Using the "bio-heat transfer" equation, and the model shown in FIGURE D2, the temperature distributions in the source-free regions can be described by Bessel functions. Qualitatively, it is found that the rate of temperature fall-off away from areas of direct insonation is proportional to a geometric term (related to the "size" of the model shown in FIGURE D2) plus a perfusion term.

For example, the two theoretical curves shown in FIGURE D1 differ from one another only by a perfusion term. For the *in vivo* calculated curve, a ratio of blood perfusion rate/tissue thermal conductivity of 1.2 cm^{-2} was assumed.

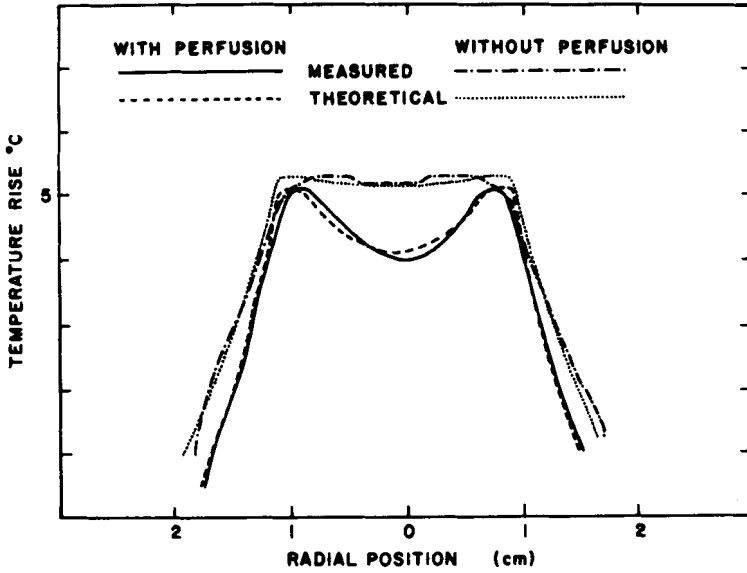


FIGURE D1.

J. SUBJECK (*Roswell Park Memorial Institute, Buffalo, N.Y.*): The intention of this work was to determine temperature distributions in tissue exposed to 434-MHz microwave radiation and to compare this with data obtained at 915 MHz, which has been long in use at this center. These measurements were performed in the pig because of the similarity between pig and human systems.

A pig was anesthetized initially with xylazine (Rompum) and later maintained under anesthetic with pentobarbital sodium through an intravenous catheter in the ear. Five copper-constantine thermocouples were inserted into the flank of the pig.

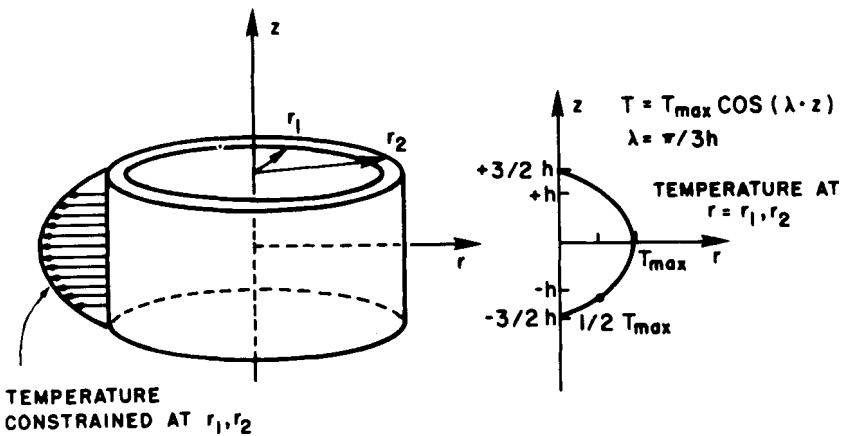


FIGURE D2. Moving transducer steady-state temperature distribution model.